자외선B 조사에 의한 모발 외부와 내부의 광산화에 관한 분광학적 비교

하병조[†]

을지대학교 미용화장품과학과
(2020년 3월 11일 접수, 2020년 3월 20일 심사, 2020년 3월 25일 채택)

Spectroscopic Comparison of Photo-oxidation of Outside and Inside of Hair by UVB Irradiation

Byung-Jo Ha[†]

Department of Beauty & Cosmetic Science, Eulji University, Sanseong-Daero 553, Sujeong-gu, Seongnam-si, Gyeong gi-do 13135, Korea
(Received March 11, 2020; Revised March 20, 2020; Accepted March 25, 2020)

초 록

모발은 여러 가지 아미노산들을 포함하는 단백질로 이루어져 있다. 자외선(UV)은 태양광선중에서 모발손상에 가장 큰 영향을 미치며 모발 노화에 주된 역할을 한다. 본 연구의 목적은 전자현미경(SEM), 공초점현미경(CLSM) 및 적외선 현미경분광법(IR micro spectroscopy)을 이용하여 정상모발에 UVB를 조사한 후 특징적인 형태학적 및 화학적 구조 변화를 알아보는 것이다. 에너지 분산형 X선 분광기가 부착된 전자현미경은 자외선 조사모발의 표면이 정상모발과 비교했을 때 거칠고 높은 산소원소의 함량을 보였다. 형광 및 3차원 위상 이미지를 CLSM으로 분석한 결과 정상모발의 초록색 형광방출이 UVB 조사모발에 비해 매우 높았다. 또한 fluorescamine 형광 염색법을 통해 UVB 조사모발은 정상모발에 비해 펩타이드 결합의 파괴로 생성된 자유 아미노기가 많음을 확인할 수 있었다. UVB 조사모발의 강한 푸른색 형광은 아미노기의 함량이 높다는 것을 의미하며, 이는 CLSM에서도 관찰되었다. 따라서 fluorescamine은 UVB 조사모발에서 펩타이드 결합의 파괴를 관찰하는데 유용한 도구가 될 수 있다. 정상모발과 UVB 조사모발의 단면을 IR micro-spectroscopy를 통해 이미지 맵핑(mapping)한 결과, UVB 조사모발은 정상 모발에 비해 모발의 표면은 물론 내부에 걸쳐 디설파이드 결합(disulfide bond)의 산화가 일어나고 있음을 확인할 수 있었다. 이러한 분광학적 방법은 단독 또는 다른 분석법과 함께 모발화장품의 개발에 응용될 수 있을 것이다.

Abstract

Hair is made of proteins containing various amino acids. Ultraviolet (UV) radiation is believed to be responsible for the most damaging effects of sunlight, and also plays an important role in hair aging. The purpose of this study was to investigate the changes in morphological and chemical structures after ultraviolet B (UVB) irradiation of human hair. The UVB-irradiated hair showed characteristic morphological and structural changes, compared to those of the normal hair. The result from a scanning electron microscope (SEM) equipped with an energy dispersive X-ray diffractometer (EDX) showed that the scale of UV-irradiated hair appeared to be rough and the amount of oxygen element was higher than that of the normal hair. Fluorescence and three dimensional (3D) topographical images were obtained by a confocal laser scanning microscope (CLSM). In 3D images, the green emission intensity of normal hair was much higher than that of fluorescing UVB-irradiated hair. The intensity of green emission reflects the intrinsic fluorescence of hair protein. Also, a fluorescent imaging method using fluorescamine reagent was used to identify the free amino groups resulting from a peptide bond breakage in UVB-irradiated hair. Strong blue fluorescence of UVB-irradiated hair, which indicates a very high level of amino groups, was observed by CLSM. Therefore, the fluorescamine as an extrinsic fluorescence could provide a useful tool to identify the peptide bond breakage in UVB-irradiated hair. Infrared image mapping was also employed to assess the cross-sections of normal and UVB-irradiated specimens to examine the oxidation of disulfide bonds. The degree of peak areas with strong absorbance for the disulfide mono-oxide was spread from the outside to the inside of hair. The spectroscopic techniques used alone, or in combination, launch new possibilities in the field of hair cosmetics.

Keywords: ATR-FTIR image, CLSM, Fluorescamine, SEM, UVB irradiation

† Corresponding Author: Eulji University,
  Department of Beauty & Cosmetic Science, Sanseong-Daero 553, Sujeong-gu,
  Seongnam-si, Gyeong gi-do 13135, Korea
  Tel: +82-31-740-7246   e-mail: bjha@eulji.ac.kr

1. Introduction

Hair is made of protein, a polymeric material based on as protein structure containing various amino acids. The amino acid compositions of hair have been reported in several studies[1]. The outstanding feature is the high disulfide bond which is considered to be specific to hair compared to other proteins[2]. The chemistry of hair is dominated by the disulfide bond formed between two protein molecules *via* inter and intra cross-linkages. The cross-section of hair is made up of three layers: an outer cuticle, cortex, and inner medulla[3]. The cuticle is the transparent outer layer of hair. It consists of many flat scales that overlap and protect the inner part of the hair. The cuticle also contains a higher concentration of disulfide bond than whole hair proteins. Also, the matrix in the cortex, referred to as the amorphous region has high sulfur and correspondingly high disulfide bond.

The decrease in the ozone layer has resulted in an increase in ultra violet (UV) irradiation reaching the Earth's surface. UV is generally believed to be largely responsible for the most damaging effects of sun light. UV may play an important role in skin aging. It has been reported that skin aging is directly related to reactive oxygen species (ROS). ROS is responsible for some of the deleterious effects of UV irradiation on skin. In particular, ROS can be mainly formed by UVB (290~320 nm). UVB irradiation leads to the photo-oxidation of tryptophan which is an aromatic amino acid[4]. The strong interest in photo-oxidation is reflected in the increasing number of scientific studies on it[5]. Photochemical degradation of hair protein results in an attack on polypeptide chains. Important modifications of hair caused by bleaching have already been reported[6], but subtle photochemical changes of in the outside and inside of hair have hardly been assessed, until now. Thus, the aim of this work was to quantify the effect of UVB irradiation on hair.

2. Materials and Methods

2.1. Hair samples

Hair samples were collected from virgin hair obtained from a South Korean female aged 20 yrs, which were presumed to be healthy. The hair was cut into 1 cm length starting approximately 5 cm from the root. The collected hair samples were washed with 1% Triton X-100 (Sigma-Aldrich, USA) to remove impurities, thoroughly rinsed with deionized water, and left to air dry.

2.2. UVB irradiation of hair sample

UV irradiation was conducted with the hair samples using a Vilber-Lourmat device (Marne-la Vallee, France) with an emission spectrum of 280~370 nm and a maximum peak at 312 nm as a UVB source. They are designed for the accurate and direct measurement of UVB irradiation. The UVB doses were assessed using a Vilber-Lourmat VLX-3W radiometer attached to a silicon photoelectric UV-CX sensor (model CX-312) for a direct measurement of UVB intensity. The UVB-irradiated samples were exposed for 6 h, at 0.55 kJ/cm^2.

2.3. Cross-section of hair sample

For cross-sectioning hair specimens, multiple short hair segments were arranged parallel in a bundle, and wrapped in threads. The wrapped hair was transferred into melted paraffin at 60 ℃ for 30 min. After final orientation of the samples, regular blocks were prepared. Serial sections (2~6 μm) of paraffin block were cut with a fresh sharp razor blade edge in a special holder attached to a regular microtome.

2.4. Staining with fluorescence

Florescamine, 4-phenylspiro[furan-2(3H)-1'-phthalan]-3,3'-dione, having the lase excitation of 390 nm, was used for labelling free amino groups and was purchased from Sigma-Aldrich Co. (USA). 10 mg of hair samples were immersed for 1 h in 5 mL of 0.05 Wt% solution of fluorescamine was prepared by dissolving in dimethyl sulfoxide (Sigma-Aldrich, USA), and 1 mL of the stock solution was added to each (5 mg), and it was mixed by vortex mixer for 5 min. Then the solution was allowed to incubate at room temperature for 15 min with shaking. The samples were collected at the bottom of the tube by centrifugation.

2.5. SEM-EDX analysis

Hitachi S-4700 (FE-SEM, Hitachi, Japan) including a Bruker AXS Quantax 4010 energy dispersive X-ray spectrometer (EDS) was used to show the morphology of hair samples without gold coating, and the semi quantification elemental analyses were performed to identify the weight percentage of major and minor elements present in the samples. Hair samples were placed on the measuring table of EDX equipment. Measurements were taken at intervals of 0.1 eV. Each peak was then quantitated for the respective elemental analysis.

2.6. Confocal laser scanning microscopic analysis

LSM 510 (Carl Zeiss, Germany) confocal laser scanning microscope was used for optical sections. 3D topographic images were obtained by using the CLSM with a 488 nm argon laser, equipped with META (Carl Zeiss, Germany). A dry 100X objective was selected, providing a resolution of approximately 0.25 μm in X, Y, and Z. The monitored stage was computer controlled to automatically reposition the sample. 3D visualization was carried out using the 3D projection module in the freeware version of the Zeiss LSM Image Browser software.

2.7. ATR-FTIR image mapping

The ATR-FTIR spectra and images were obtained using a micro-FTIR system (FTIR 6200, Jasco, Japan), and a mercury-cadmium-telluride (MCT) detector with 16 linear arrays. This system had a spectral resolution of 8 cm^{-1}, and was averaged to obtain areas on an able signal-to-noise ratio. The wave number ranged from 4,000 cm^{-1} to 750 cm^{-1}. Analysis was performed in absorbance mode using the microscope. The position and focus of the samples were adjusted microscopically through an aperture in the ATR-FTIR optical section.

Table 1. Elemental Analysis Data of Normal Hair and UVB-Irradiated Hair   (unit: Wt%)

Items	C	O	S
Normal hair	56.76	41.70	1.54
UVB irradiated hair	54.52	44.30	1.18

(a)

(b)

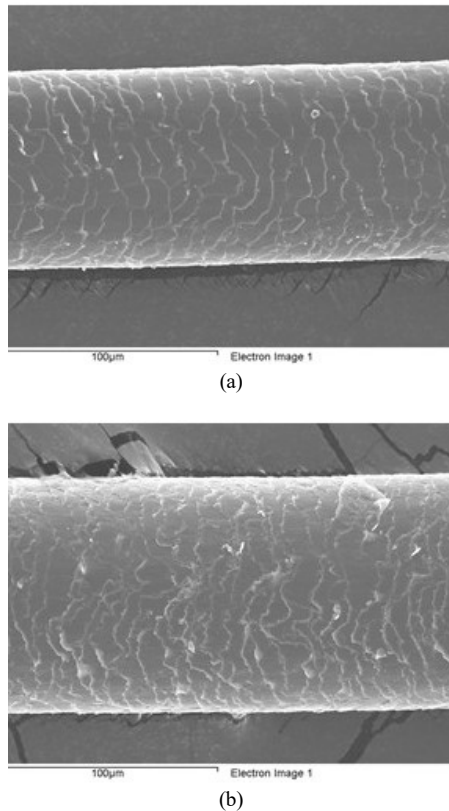**Figure 1. SEM images of normal hair and UVB-irradiated hair. (a) normal hair, (b) UVB-irradiated hair.**

(a)

(b)

Figure 2. EDX element composition of normal and UVB-irradiate hair. (a) normal hair, (b) UVB-irradiated hair.

3. Results and Discussion

3.1. Analysis of hair by SEM-EDS

The cuticle cells, derived from normal hair, form a sequenced and continuous cuticle pattern[7]. UVB-irradiated hair presents a more severe lifting up compared to normal hair, with the loss of tightly overlapping cuticle scales. A less uniform surface confirmed the chemical oxidation of the cuticle. Figure 1 shows SEM images of normal hair and UVB irradiated hair. The surface of the normal hair appears to be smoother than UVB-irradiated hair. This unusual lifting of the surface could be explained by local resistance of the cuticle scales[8]. The changes in the cuticle surface caused by UVB-irradiated hair were similar to those of chemical bleaching[6]. Changes in the frictional properties due to cuticle damage determine how hair feels to the touch.

The normal hair and UVB-irradiated hair were analyzed by EDX. The EDX analysis is presented in Table 1. A larger quantity of carbon and oxygen elements were found while sulfur was less[9]. In particular, the pe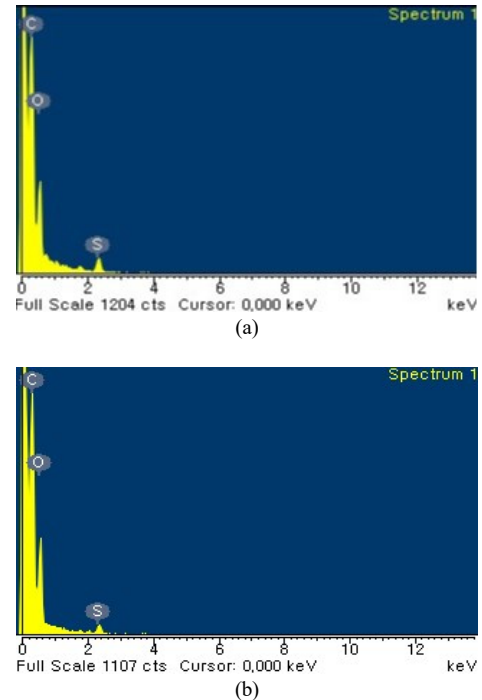rcentage of carbon was higher when compared to other elements. The second highest quantity in human hair is oxygen. It is interesting to note the normal hair has a higher sulfur content of sulfur than UVB-irradiated hair. Hair damage can be defined as a decrease in disulfide bonds[10]. Sulfur is the important element in human hair, and is suggested to have an role in the maintenance of hair structure[11]. The interesting feature is that, in normal hair, the quantity of oxygen is lower compared with the UVB-irradiated hair. The relatively high oxygen content is caused by the oxidation of disulfide bonds. This oxidation in protective cuticle cells allows the splitting of the hair and facilitates further damage.

3.2. Analysis of hair by CLSM

CLSM offers a breakthrough from the classic observation of the hair in SEM. CLSM also offers several advantages over conventional wide-field microscopy, most important of which are the production of high quality and the capability to collect serial optical sections from thick specimens up to 100 μm[12]. By using CLSM, the hair can be observed in its natural environment with less damage than by other microscopic methods[13,14]. As shown in Figure 3, normal hair issued a high green emission by auto-fluorescence of hair protein, which is regularly spaced along the hair shaft. The higher fluorescence of normal hair revealed more aromatic amino acids than regularly spaced along the hair shaft. Hair exhibiting fatigue after oxidative stress showed hazy cuticle borders and lacked the regular spacing between cells[15]. UVB irradiation is mainly responsible for hair cuticle damage as well as the responsible for the oxidative degradation of aromatic amino acids such as tryptophan, tyrosine, and phenylalanine. To study the effect of UVB on the surface morphology of hair, a 3D re-
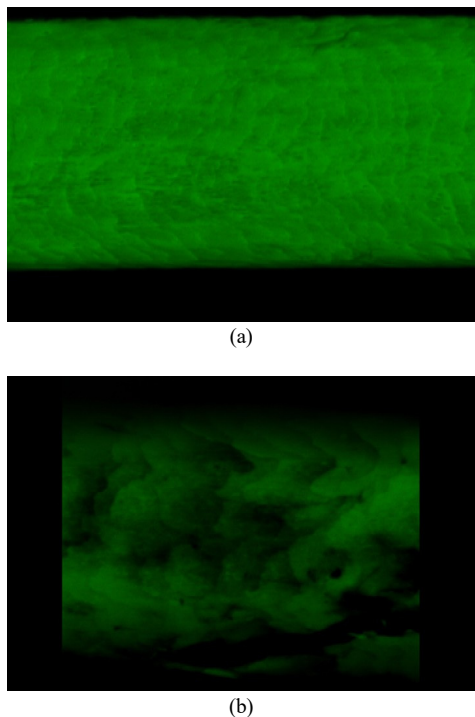
Figure 3. CLSM surface picture of normal hair and UVB-irradiated hair. (a) normal hair, (b) UVB-irradiated hair.

Figure 4. 3D reconstructions on the insides of normal hair and UVB-irradiated hair. (a) normal hair, (b) UVB- irradiated hair.

construction of CLSM auto-fluorescence was conducted to examine the internal hair structure. The optical sectioning property of CLSM can be conveniently applied to observe internal hair structure[16]. The endo-morphology of the hair is shown in Figure 4, which is a reconstruction of a subset of optical slices that allows for the visualization of internal structures. As shown in Figure 4, the inner structure before UVB irradiation showed that the interface is bumpy and the interface area is high. As a result, more green fluorescence was emitted.

However, after UVB radiation the inner structure showed that the interface of the internal structure is less bumpy and the interface area is low. This difference in endo-morphology after UVB irradiation was due to the breakage of aromatic amino acids in hair protein[6]. An optical sectional view was observed in the 3D images, with respect to the inner shapes[17]. Characteristic green fluorescence was observed in normal hair, while in UVB-irradiated hair green fluorescence was disappeared. It is speculated that ROS occurring on the surface of hair affects the morphology depending on the contents of disulfide mono-oxides and aromatic amino acids.

3.3. Analysis of hair by fluorescence probe

Another important field of investigation uses fluorescence probes which reveals the internal functional group of hair. Fluorescence probes specific to free amino groups have been developed and are used in conjunction with microscopy[18]. Fluorescamine as a fluorescence probe is relatively small molecule that show changes in one of its fluorescence properties as a result of interaction with their molecular environment, and can serve as a useful tool to detect the free amino groups [18]. Such interaction may be related to covalent binding to the func-
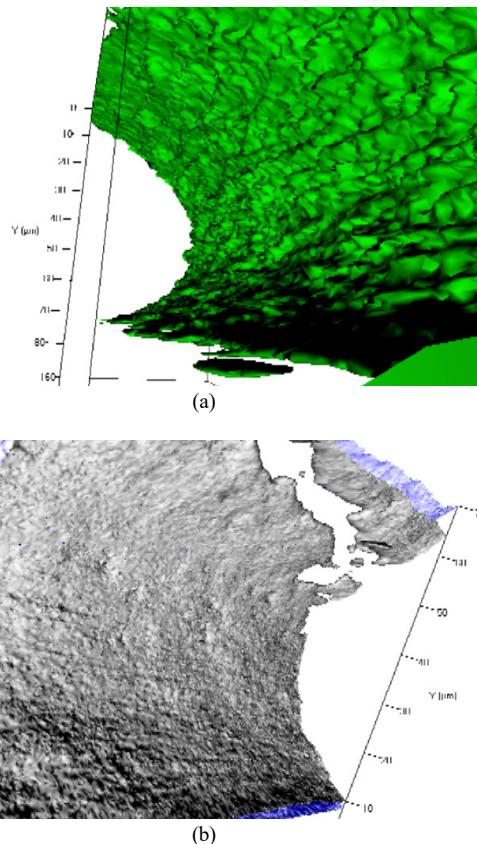
tional group of a protein[19]. As shown in Figure 5, fluorescamine increased the contrast of the blue emission in UVB-irradiated hair. The increase in blue fluorescence reflects the rise in free amino groups resulting from peptide bond breakage[18]. This allows a greater selection for UVB-irradiated hair. The corresponding blue fluorescence demonstrated the existence of the free amino groups on the surface of the hair.

As shown in Figure 5, normal hair is less fluorescent, but UVB- irradiated hair undergoes fluorescent enhancement and a large absorption and emission blue shift. These results indicate that the free amino groups are more abundant in UVB-irradiated hair. UVB-irradiated hair was found to react as easily as the free amino groups, facilitating the breakage of peptide bonds. The results obtained indicated that fluorescamine reaction with UVB-irradiated hair is a useful histochemical procedure for collecting an information on chemical changes in hair protein[20].

3.4. Analysis of hair by IR micro spectroscopy

IR image mapping was employed to assess thin cross-sections of normal and UVB-irradiated hair to comprehend the photo-oxidation of hair. Transformations due to the photo-oxidation of disulfide bonds were observed and spatially characterized[20,21]. Spectral mapping of infrared functional groups could demonstrate how the oxidation reaction spread throughout the cortex[22,23]. Figure 6a shows dis-
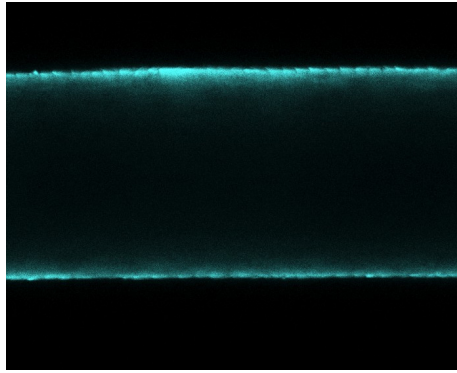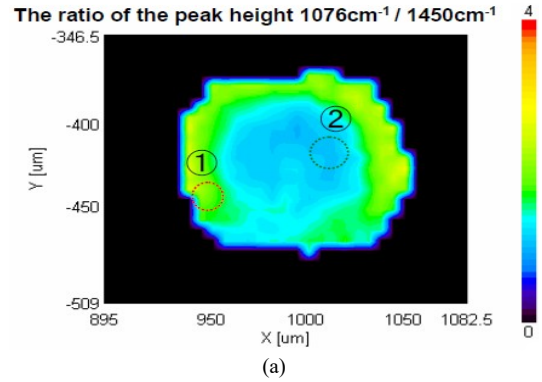
(a)
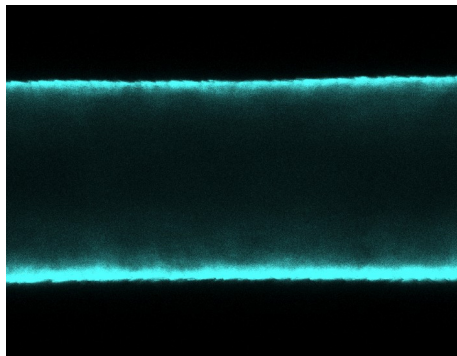
(b)

Figure 5. Fluorescence images by using fluorescamine probe. (a) normal hair (b) UVB-irradiated hair.
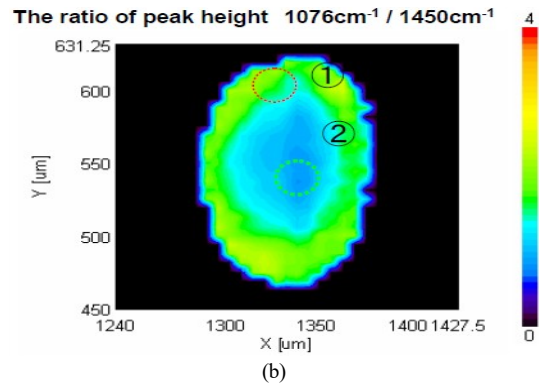

(a)

(b)

Figure 6. (a)IR micro-spectroscopic image mapping on the ratio of peak height 1,076 cm⁻¹/1,450 cm⁻¹. ① outside normal hair, ② inside normal hair. The numbers show the micro-areas analyzed. (b) IR micro-spectroscopic image mapping of the ratio of peak height 1,076 cm⁻¹/1,450 cm⁻¹. ① outside of UVB-irradiated hair, ② inside of UVB-irradiated hair. The numbers show the micro-areas analyzed.

tribution mapping of disulfide mono-oxide in cross-sectioned normal hair. A wavelength of 1,076 m^{-1} is typically associated with disulfide mono-oxide. The peak intensity of mono-oxide was ratioed with a methylene peak at 1,450 cm^{-1} as an internal reference, which was chemically unchanged during the oxidation process. Therefore, a ratio of 1,076 cm^{-1}/1,450 cm^{-1} is an indication of the degree of disulfide oxidation[24,25]. As shown in Figure 6a, the disulfide mono-oxide peak intensity on the outside of hair was much higher than inside hair. This result was good agreement with Figure 7a. The absorbance peak due to disulfide mono-oxide can be seen in the outer region of the cuticle to the cortex, indicating that the hair was significantly attacked by several environmental factors from the cuticle to the cortex[26,27]. The daily exposure of normal hair to sunlight is one of the environmental factors[28]. As shown in Figure 6a, the area of mono-oxide peak intensity of UVB-irradiated hair was much larger than that of normal hair, indicating that most of the cuticle layer changed to an oxidized form by UVB irradiation. In Figure 7b, ATR-FTIR spectrum shows that the outside of the cross-section of UVB-irradiated hair exhibits much higher oxidization than that of the inside of the cross-sectioned normal hair[26]. An areas with strong absorbance for disulfide mono-oxide were spread throughout the cortex region.

4. Conclusion

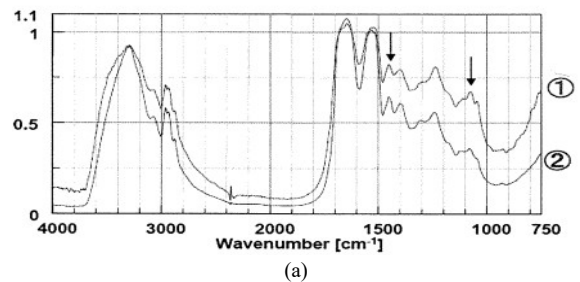In this paper, three different analytical methods were applied to eval-
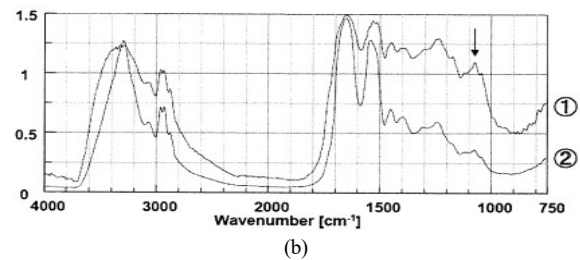

(a)

(b)

Figure 7. (a) ATR-FTIR spectrum of normal hair. ① outside hair, ② inside hair. In the ordinate, absolute absorbance values are reported. Each arrow means the absorbance peaks at 1,450 cm⁻¹ and 1,076 cm⁻¹. (b) ATR-FTIR spectrum of UV-irradiated hair. ① outside hair, ② inside hair. In the ordinate, absolute absorbance values are reported. The arrow means the absorbance peak at 1,076 cm⁻¹.

uate photo-oxidation with respect to the surface morphology, fluorescence, and chemical structural changes of hair. SEM-EDX was applied to examine the surface morphology together with the elemental composition. The observation of morphology showed that the UVB-irradiated hair appeared to have a loose packing of surface scales, lower ratio of sulfur content and higher ratio of oxygen element. The natural fluorescence of hair as a bio-marker can be used to study various processes from the damages of photo-oxidation. Optical slices made with CLSM showed the location of fluorescing processes. Changes in fluorescing compounds depend on the state of hair. Both the surface and the internal structure can be imaged non-destructively, thus providing longitudinal and transversal optical sections, In the auto-fluorescence CLSM, the green emission intensity of normal hair reflects the intrinsic fluorescence of hair protein containing aromatic amino acids. UVB irradiation induced significant loss of aromatic amino acids. In the optical section by using CLSM, high auto-fluorescent intensity appeared in normal hair. This showed that aromatic amino acids that can be auto-fluorescent were more abundant than UVB irradiated hair. Auto-fluorescence seen with CLSM could thus provide an invaluable non-invasive tool to study the state of hair proteins for a wide range of conditions. Fluorescamine as an extrinsic fluorescence probe was useful to detect the free amino groups resulting from peptide bond breakage. IR image mapping suggested that the outside of hair exhibits much higher oxidation than the inside. ATR with FTIR was also useful to provide functional group image mapping. Both methods, CLSM and ATR-FTIR, were found to be suitable to analyze photo-oxidation by UVB irradiation. To date, non-destructive spectroscopic imaging mode have not been compared directly by combining other analytical spectroscopic methods for human hair. Therefore, combining spectroscopic methods could supplement each other to exact additional information from the state of hair.

References

1. A. H. Powitt, *Hair Structure and Chemistry Simplified*, Milady Publishing Corp., New York (1970).
2. C. R. Robbins, *Chemical and Physical Behavior of Human Hair*, 4th Edition, Springer Verlag, New York (2002).
3. D. P. Harland, R. J. Walls, J. A. Vernon, J. M. Dyer, J. L. Woods, and F. Bell, Three dimensional architecture of macrofibrils in the human scalp hair cortex, *J. Struct. Biol.*, **185**, 397-404 (2014).
4. J. M. Dyer, J. E. Plowman, G. I. Krsinic, S. Deb-Choudhury, H. Koehn, K. R. Millington, and S. Clerens, Proteomic evaluation and location of UVB-induced photo-oxidation in wool, *J. Photochem. Photobiol. B. Biol.*, **98**, 118-127 (2010).
5. C. M. Pande and J. Jschowicz, Hair photodamage-measurement and prevention, *J. Soc. Cosmet. Chem.*, **44**, 109-122 (1993).
6. B. J. Ha, Instrumental analysis of the human hair damage by bleaching treatments, *J. Fashion Business*, **12**, 23-33 (2008).
7. B. K. Filshie and G. E. Rogers, An electron microscope study of the structure of feather keratin, *J. Cell Biol.*, **13**, 1-12 (1962).
8. L. J. Wolfram and M. K. O. Lindermann, Some observations on hair cuticle, *J. Soc. Cosmet. Chem.*, **22**, 839-850 (1971).
9. R. C. Clay, K. Cook, and J. I. Routh, Studies on the composition of human hair, *J. Am. Chem. Soc.*, **62**, 2709-2710(1940).
10. D. Sanford and F. L. Humoller, Determination of cystine and cysteine in altered human hair fibers, *Anal. Chem.*, **19**, 404-406(1947).
11. J. H. Bradbury, The structure and chemistry of keratin fibers, *Adv. Protein Chem.*, **27**, 111-211(1973).
12. J. M. Lagarde, P. Peyre, D. Redoules, D. Black, M. Briot, and Y. Gall, Confocal microscopy of hair, *Cell Biol. Toxicol.*, **10**, 301-304 (1994).
13. M. Rajadhyaksha, S. Gouzalez, J. M. Zavislan, R. R. Anderson, and R. H. Webb., In vivo confocal scanning laser microscopy of human hair II, *J. Invest Dermatol.*, **113**, 293-303 (1999).
14. A. Nwaneshiudu, C. Kuschal, F. H. Sakamoto, R. Anderson, K. Schwarzenberger, and R. C. Younger, Introduction to confocal microscopy, *J. Invest. Dermatol.*, **132**, 1-5 (2012).
15. C. M. Pande and J. Jachowicz, Hair photodamage measurement and prevention, *J. Soc. Cosmet. Chem.*, **44**, 109-122 (1993).
16. M. Rajadhyaksha, S. Gouzalez, D. Esterowitz, R. H. Webb, and R. R. Anderson, *In vivo* confocal scanning laser microscopy of human hair; Melanin provides string contrast, *J. Invest. Dermatol.*, **104**, 946-952 (1995).
17. P. Corcuff, P. Gremillet, M. Jourlin, Y. Duvaukt, F. Leroy, and J. L. Leveque, 3D reconstruction of human hair by confocal microscopy, *J. Soc. Cosmet. Chem.*, **44**, 1-12 (1993).
18. S. Udenfriend, S. Stein, P. Bohlen, W. Dairman, W. Leimgruber, and M. Weigele, Fluorescamine: A reagent for assay of amino acids, peptides, proteins, and primary amines in the picomole range, *Science*, **178**, 871-872 (1972).
19. A. M. Felix and M. H. Jimenez, Rapid fluorometric determination for completeness in solid phase coupling reactions, *Anal. Biochem.*, **52**, 377-381(1973).
20. M. Zielinski, A new approach to hair surface topography: Fourier transform and fractal analysis, *J. Soc. Cosmet. Chem.*, **40**, 173-189 (1989).
21. M. A. Mujeeb and M. K. Zafar, FTIR spectroscopic analysis of human hair, *Int. J. Innovative Res. in Sci. Eng. and Tech.*, **6**, 9327-9332(2017).
22. D. J. Lyman and J. Murray-Wijelath, Fourier transform infrared attenuated total refraction analysis of human hair: Comparison of human hair from breast cancer patients with hair from healthy subjects, *Appl. Spectrosc.*, **59**, 26-32 (2005).
23. W. Akhtar, H. G. Edwards, and D. W. Farwell, Fourier-transform raman spectroscopic study of human hair, *Spectrochim. Acta, Part A. Mol. Biomol. Spectrosc.*, **53**, 1021-1031 (1997).
24. C. M. Carr and D. M. Lewis, An FTIR spectroscopic study of the photodegradation and thermal degradation of wool, *J. Soc. Dye. Colour*, **109**, 21-24 (1993).
25. M. Joy and D. M. Lewis, The use of Fourier transform infra-red spectroscopy in the study of the surface chemistry of hair fibres, *Int. J. Cosmet. Sci.*, **13**, 249-261 (1991).
26. J. Strassburger, Quantitative fourier transform infrared spectroscopy of oxidized hair, *J. Soc. Cosmet. Chem.*, **36**, 61-74 (1985).
27. V. Signori and D. M. Lewis, FTIR investigation of the damage produced on human hair by weathering and bleaching processes: Implementation of different sampling techniques and data processing, *Int. J. Cosmet. Sci.*, **19**, 1-13 (1997).
28. R. Mendelsohn, M. E. Rerek, and D. J. Moore, Infrared spectroscopy and microscopic imaging of stratum corneum models and skin invited lecture, *Phys. Chem. Chem. Phys.*, **2**, 4651-4657 (2000).